Novel Citric Acid-Based Biodegradable Elastomers for Tissue Engineering**

By *Jian Yang*, *Antonio R. Webb*, and *Guillermo A. Ameer**

Tissue engineering often requires the use of a three-dimensional scaffold for cells to grow on and differentiate properly. Generally, the ideal scaffold should be biocompatible, biodegradable, allow for adequate cell loading, facilitate cell proliferation and differentiation, and possess mechanical and physical properties that are suitable for the target application.[1–3] As many tissues in the body have elastomeric properties, successful tissue engineering will require the development of compliant biodegradable scaffolds.[4] Despite the recognized importance of mechanical stimuli on tissue development, there has been a dearth of research on the design and evaluation of elastomeric biodegradable scaffolds.[5–10] The few materials that have been reported in the literature require complex and costly synthesis procedures, which translate into higher manufacturing costs and hinder the commercial and clinical implementation of tissue engineering.[11–20] Herein we describe the synthesis and characterization of a novel biodegradable elastomer, poly(1,8-octanediol-*co*-citric acid) (POC), which has potential for use in tissue engineering, in particular the engineering of small-diameter blood vessels. Development of materials for this application is important as cardiovascular disease affecting blood vessels is the principal cause of death in the USA.[21] POC has the following advantages: non-toxic monomers, a relatively simple synthesis that can be carried out under mild conditions without addition of toxic catalysts or crosslinking reagents (making it a good candidate for drug delivery and cost-effective scale-up), controllable mechanical and biodegradation properties, easy processing, and inherent surface affinity for various cell types.

The rationale behind POC was to react the polyfunctional monomer citric acid with the difunctional monomer 1,8-octanediol to create a polyester network with a controllable number of crosslinks, in order to tailor the elasticity and biodegradability of the resulting material. Citric acid was chosen as a polyfunctional monomer because it is a non-toxic metabolic product of the body (Krebs or citric acid cycle), it is readily available, and inexpensive. It is also a reactive monomer that can participate in hydrogen bonding interactions within a polyester network. 1,8-octanediol was chosen as the difunctional monomer to enable ester bond formation with citric acid and because it is the largest aliphatic diol that is water-soluble with no reported toxicity, a property that should be beneficial to the degradation process (leaving no remaining insoluble complexes). We first synthesized a pre-polymer by carrying out a controlled condensation reaction between 1,8-octanediol and citric acid. The pre-polymer, whose weight-average molecular weight (M_w) is 1088 ($M_n = 1085$), can be purified via precipitation in water followed by freeze-drying, or used as is for further post-polymerization or crosslinking. An intense C=O stretch at 1735 cm^{-1} in the Fourier transform infrared (FTIR) spectra of purified POC pre-polymer confirms the formation of ester bonds.[4] The pre-polymer can be dissolved in several solvents including ethanol, acetone, dioxane, and 1,3-dioxolane, facilitating subsequent processing into various scaffold geometries. The ^1H NMR spectra of purified POC pre-polymer confirms that the composition of the pre-polymer is approximately 1:1 citric acid/1,8-octanediol, which agrees with the initial reaction feed monomer ratio.

Synthesis of POC is simple and can be conducted under very mild conditions, a significant advantage when compared to existing biodegradable elastomers. For example, we have crosslinked the pre-polymer at 80 °C, 60 °C, and even 37 °C, at atmospheric pressure. This creates the possibility of utilizing POC as a drug (protein) delivery vehicle, since the low crosslinking temperature can help maintain the stability and activity of POC-entrapped drug or protein. Crosslinking POC at these temperatures also leads to a low degree of crosslinking and a relatively high molecular weight between crosslinks, characteristics that are conducive to the high elongation and low modulus typical of elastomers. Despite the selection of 1,8-octanediol for this study, we have successfully synthesized other elastomers with alternative aliphatic diols (Fig. 1A) and polyethylene oxides (data not shown). Therefore, citric acid can be used as a polyfunctional crosslinking monomer that can be reacted with diols to create degradable elastomeric materials. The mechanical properties of the elastomer can be modulated by controlling synthesis conditions such as crosslinking temperature and time, vacuum, and initial monomer molar ratio, as explained below. The low cost of the monomers and the simple methods for synthesis of POC should also increase its potential for future commercialization.

POC is a strong elastomeric, biodegradable, and hydrophilic "cell-friendly" material. Tensile tests produced a stress–strain curve characteristic of an elastomeric material (Fig. 1B). Ultimate tensile strengths were as high as 6.1 ± 1.4 MPa and the Young's moduli ranged from 0.92 ± 0.02 to 16.4 ± 3.4 MPa. These values are comparable to those of elastin from bovine ligament (tensile strength and Young's modulus of 2 MPa and 1.1 MPa, respectively).[22] The maximum elongation at break was 265 ± 10 % of initial length, similar to that of arteries and veins (up to 260 %)[23] and elastin (up to 150 %).[22] The results in Table 1 indicate that increased crosslinking temperatures and time increase the tensile strength and Young's modulus while decreasing the elongation at break, (though all ultimate elongation values are at least 100 % of original length). No crystallization or melting

[*] Prof. G. A. Ameer, Dr. J. Yang, A. R. Webb
Room E310, Biomedical Engineering Department
Northwestern University
2145 Sheridan Rd., Evanston, IL 60208 (USA)
E-mail: g-ameer@northwestern.edu

[**] The authors thank Maisha Gray from the Torkelson Lab for her help in obtaining the GPC data. This work was funded in part through a grant by the American Heart Association and the National Institutes of Health (R21-HL071921–02)

DOI: 10.1002/adma.200306264

ADVANCED MATERIALS

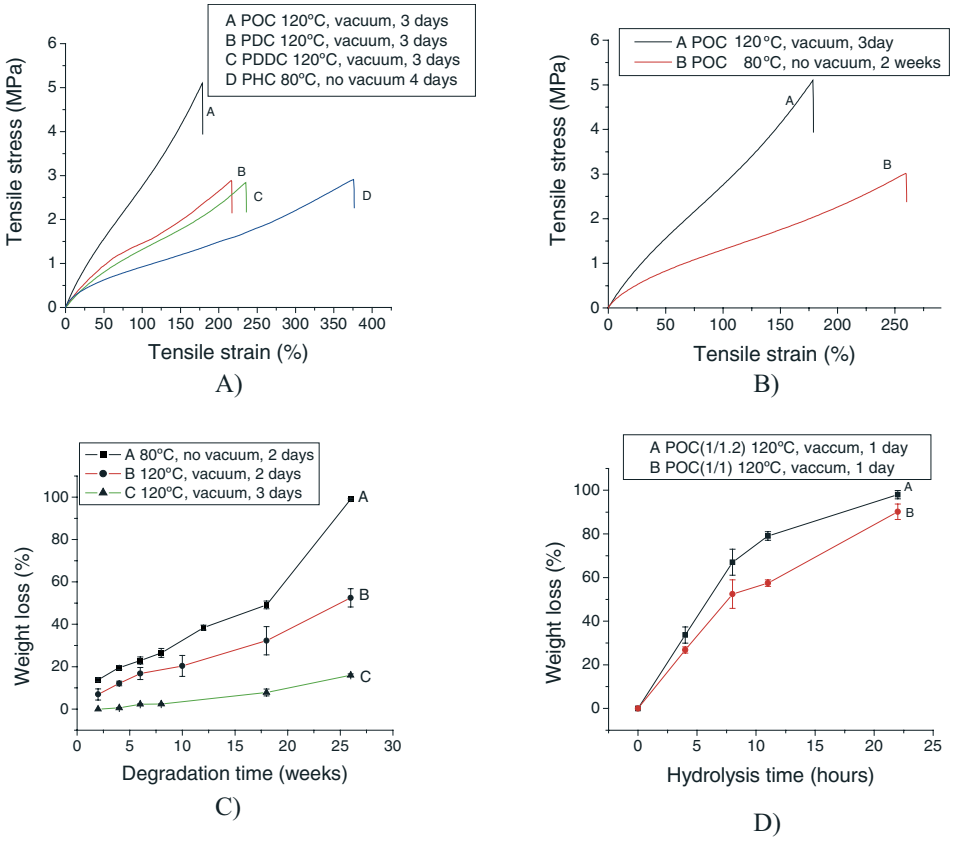

Figure 1. A) Typical stress–strain curve of POC, PDC (poly(1,10-decanediol-*co*-citric acid)), PDDC (poly(1,12-dodecanediol-*co*-citric acid)), and PHC (poly(1,6-hexanediol-*co*-citric acid)) elastomers, all with monomer ratios of 1:1 diol/citric acid. B) Stress–strain curves of POC (molar ratio: 1,8-octanediol/citric acid = 1:1) synthesized under different reaction conditions; C) mass loss of POC (1,8-octanediol/citric acid = 1:1) degraded in PBS at 37 °C for 26 weeks; and D) mass loss of POC with monomer mole ratio of 1:1 1,8-octanediol/citric acid (tensile stress = 3.62±0.32 MPa, Young's modulus = 2.84±0.12 MPa, active network chain segment per unit volume, n = 375.77±15.88 mol m^{-3}) and 1:1.2 1,8-octanediol/citric acid (tensile stress = 3.10±0.22 MPa, Young's modulus = 3.24±0.26 MPa, active network chain segment per unit volume, n = 428.69±34.40 mol m^{-3}) degraded in 0.1 M NaOH.

Table 1. Mechanical properties and cross-link density of POC synthesized under different post-polymerization conditions [a].

POC	Post-polymerization condition	ρ [g/m^3] $\times 10^{-6}$	Young's modulus [MPa]	Elongation at break [%]	n [mol/m^3]	M_c [g/mol]
1	120°C, 2 Pa 1 day	1.24±0.082	2.84±0.12	253±19	375.77±15.88	3301±218
2	120°C , 2 Pa 3 day	1.28±0.056	4.69±0.48	160±15	620.68±63.51	2068±90
3	120°C , 2 Pa 6 day	1.31±0.10	6.44±0.28	117±14	852.10±37.05	1543±117
4	80°C , 14 day	1.25±0.028	2.66±0.15	265±10	351.95±19.85	3542±78

[a] ρ: polymer density; n: the number of active network chain segment per unit volume; M_c: the molecular weight between cross-links; monomer mole ratio: 1:1.

temperatures are observed in thermograms obtained via differential scanning calorimetry. An apparent glass transition temperature (T_g) is observed below 0 °C (–10 to ~0 °C). This result confirms that POC is totally amorphous at 37 °C, its expected operating temperature. An intense OH stretch at 3464 cm^{-1} in FTIR spectra suggests that the hydroxyl groups are hydrogen bonded, which can contribute to the mechanical properties.[4] The degradation of POC is modulated by changing the post-polymerization (crosslinking) temperature and time, and the molar ratio of the monomers (Figs. 1C,D). POC post-polymerized under mild conditions (low temperature, e.g., 60 °C or 80 °C, no vacuum) has a significantly faster degradation rate than that of POC post-polymerized under relatively tougher conditions (high temperature, e.g., 120 °C, 2 Pa vacuum) as it is completely degraded after 6 months of incubation in phosphate buffered saline (PBS) at 37 °C (Fig. 1C). Depending on implant location, the degradation rate may be faster in vivo due to enzymatic or cellular effects, as previously described by others,[4] and this potential issue will be the subject of further study. Nevertheless, the degradation characteristics of POC are expected to fall within the scaffold degradation time-

scales that are required of most tissue engineering applications. Since the crosslink density is directly proportional to the strength but inversely proportional to the degradation rate of POC, tailoring the properties of the elastomer would be difficult if only the crosslink density can be varied. Therefore we hypothesized that by increasing the mol-% of the more hydrophilic crosslinker we could confer flexibility on the design of POC and similar materials based on crosslinked polyester networks. Increasing the molar ratio of citric acid increases the degradation rate of the copolymer without sacrificing its initial tensile strength, likely due to the hydrophilicity and reactivity of poly(citric acid) segments and the increased number of crosslinks that are formed within the POC network (Fig. 1D). These results show that POC is a degradable copolymer and that the degradation rate can be modulated by changing post-polymerization conditions and monomer composition. To our knowledge, there are no reported materials with the properties described herein that have been synthesized via polycondensation under such mild conditions.

The hydrophilicity of a material is one of the properties that control protein deposition, cell affinity, and degradation rate. The initial water-in-air contact angles of POC post-polymerized at 80 °C and 120 °C (equal reaction time) are 57° and 76°, respectively. After 30 min, the equilibrium contact angles are 22° and 38°, respectively. The potential use of POC in cardiovascular tissue engineering led to the evaluation of its cell affinity and biocompatibility with human aortic smooth muscle cells (HASMC) and human aortic endothelial cells (HAEC). The growth and viability of each cell type is at least as good as or better than that observed on poly(L-lactic acid) films (Figs. 2A,B). Both cell types attach, display a normal phenotype, and promptly achieve confluence when cultured on POC films in low serum media (crosslinked at 80 °C or 120 °C, equal reaction time) (Figs. 2C,D). It is noted that the culture of either cell type did not require pre-coating or pre-treatment of POC with adhesion proteins such as fibronectin or laminin to facilitate cell attachment. Such pre-treatment steps are often considered essential to obtain vascular endothelial cell adhesion onto biomaterials.[24] Although POC would also mediate some degree of non-specific adsorption of proteins, additional exogenous protein coatings may increase non-specific binding of other tissue components such as platelets and increase the cost of the end product. The fact that unmodified POC can support cell adhesion and confluence without additional treatments is therefore a significant advantage. In addition, the surface of POC can be easily modified via available carboxyl or hydroxyl functional groups, if necessary. The in vivo biocompatibility of POC, crosslinked using conditions two and four in Table 1, was evaluated via subcutaneous implantation in Sprague–Dawley rats. No chronic inflammatory response was observed (Figs. 2E,F). The thickness of the fibrous capsules in both cases was approximately 45 μm, similar to that reported in the literature for another biodegradable elastomer, poly-(glycerol sebacate) (PGS), and smaller than

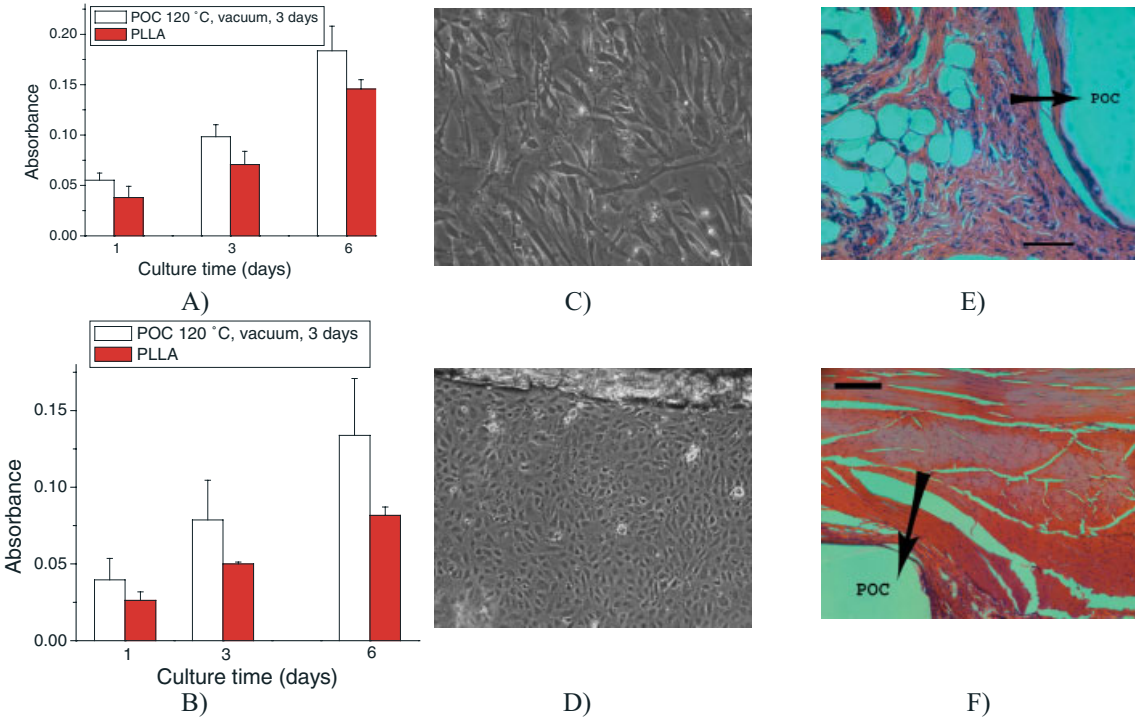

Figure 2. Biocompatibility evaluations in vitro and in vivo. Methylthiazoletetrazolium (MTT)–tetrazolium assay of HASMC (A) and HAEC (B) on POC (120 °C, 2 Pa, 3 days) and PLLA (M_w = 300 000) films. Photomicrograph (×100) of HASMC (C) and HAEC (D) cultured on POC (1/1, 120 °C, vacuum, 3 days. E) H&E staining of POC film (80 °C, no vacuum, 2 weeks), and F) H&E staining of POC film (120 °C, vacuum, 3 days) implants after 60 days of implantation, scale bar = 100 μm.

ADVANCED MATERIALS

that reported for poly(L-lactide-*co*-glycolide) (PLGA).[4] A thinner fibrous capsule is considered to be beneficial for mass transfer between a cell-based implant and surrounding tissues.

POC can be easily processed into scaffolds for vascular tissue engineering. Despite the fact that crosslinked POC can be classified as a thermoset copolymer, similar to vulcanized rubber, in pre-polymer form it can be processed into conventional scaffold geometries and microarchitectures. Tubular and sponge-like POC scaffolds with inter-connected pore structures can be fabricated using molds and the commonly used salt leaching technique (Fig. 3).[25,26] Using salt leaching, we have obtained scaffold pore sizes and porosities of 106 ± 26 μm and 90 ± 2 %, respectively. Many micropores (11 ± 3 μm) are also distributed within the macropores, a characteristic that is expected to enhance nutrient transport within the scaffold. Preliminary data suggest that porous POC scaffolds should exhibit good fatigue resistance as the Young's modulus (0.482 MPa) of cylindrical samples remained constant when subjecting the scaffolds to five hundred compression cycles in a mechanical tester. Recovery from deformation was almost 100 % after the compression cycles.

Thin-walled POC tubes (120 °C, vacuum, 1 day, 3.66 mm inner diameter, 0.15 mm wall thickness) for potential use as small-diameter vascular grafts, were compliant and had high burst strengths. The burst pressure of POC tubes was 1300 mmHg (1 mmHg = 0.0075 Pa). This burst pressure is similar to that reported for native human saphenous veins (1680 ± 307 mmHg).[27] It is noted that the bust pressures will depend on the post-polymerization conditions, the tube diameter and wall thickness. The results suggest that POC tube scaffolds may be strong enough to act as a temporary template for blood vessels engineered in vivo.

Compared to existing biodegradable elastomers in tissue engineering, POC is inexpensive and easy to synthesize and process. The biocompatibility data presented herein support the potential use of POC in tissue engineering applications as well as other clinical procedures that may require a biodegradable elastomeric implant. Material properties, such as mechanical strength, hydrophilicity, degradation rate, and cell affinity, can be tailored by modulating the monomer ratio, post-polymerization conditions, and grafting of biomolecules in order to mimic the function of elastomeric tissues.[2]

Experimental

Preparation of Poly(1,8-octanediol-co-citric acid) (POC): All chemicals were purchased from Sigma-Aldrich (Milwaukee, WI). Equimolar amounts of citric acid and 1,8-octanediol were added to a 250 ml three-neck round-bottom flask fitted with an inlet and outlet adapter. The mixture was melted under a flow of nitrogen gas by stirring at 160 °C–165 °C in a silicon oil bath, and then the temperature of the system was lowered to 140 °C. The mixture was stirred for another hour at 140 °C to create the pre-polymer solution. The pre-polymer was post-polymerized at 37 °C, 60 °C, 80 °C, or 120 °C under vacuum (2 Pa) or no vacuum for times ranging from 1 day to 2 weeks to create POC with various degrees of cross-linking. Several citric acid based elastomers were synthesized as described above using other diols. The resulting copolymers were poly(1,6-hexanediol-*co*-citric acid) (PHC), poly(1,10-decanediol-*co*-citric acid) (PDC), and poly(1,12-dodecanediol-*co*-citric acid) (PDDC).

Polymer Characterization: Fourier transform infrared spectra were obtained at room temperature using a FTS40 Fourier transform infrared spectrometer (BioRad Hercules, CA). Sample films (12 μm thick) were prepared using a microtome and placed on a KBr crystal. ^{1}H nuclear magnetic resonance (^{1}H NMR) spectra for pre-polymers were recorded on a Varian NMR spectrometer (model Mercury 400, Palo Alto, CA) at 400 MHz. The pre-polymers were purified via precipitation in water with continuous stirring followed by freeze-drying and then dissolved in dimethyl sulfoxide-d_6 (DMSO-d_6) in tubes with a 5 mm outside diameter. Composition of the pre-polymer was determined by calculating the signal intensities of $-OCH_2CH_2-$ at $\delta = 1.53$ ppm from 1,8-octanediol and $-CH_2-$ at $\delta = 2.79$ ppm from citric acid [28]. The chemical shifts in ppm for ^{1}H NMR spectra were referenced relative to tetramethylsilane (TMS, 0.00 ppm) as the internal reference. The average molecular weight of pre-polymer was determined by gel permeation chromatography (GPC) measurements on a Waters Breeze instrument equipped with three Waters columns (Styragel HMW 2, HMW 6E, and HR4) using tetrahydrofuran as the eluent and a Waters 2410 refractive index detector. Polystyrene standard was used for calibration. Differential scanning calorimetry (DSC) thermograms were recorded in the range of –80 °C to 600 °C on a DSC550 instrument (Instrument Specialists Inc. Spring Grove, IL) using a heating rate of 10 °C min^{-1}. Water-in-air contact angle was measured at room temperature using a Ramé–Hart (RHI) goniometer and imaging system (Ramé–Hart Mountain Lakes, NJ) using the sessile drop method [29]. Four independent measurements at different sites were averaged. The contact angle was monitored with time until no apparent change was detected within five minutes. Tensile tests were conducted according to ASTM D412a on an Instron 5544 mechanical tester equipped with 500 N load cell (Instron Canton, MA). Briefly, the dog-bone-shaped sample (26 mm × 4 mm × 1.5 mm, length × width × thickness) was pulled at a rate of 500 mm min^{-1}. Values were converted to stress–strain and a Young's

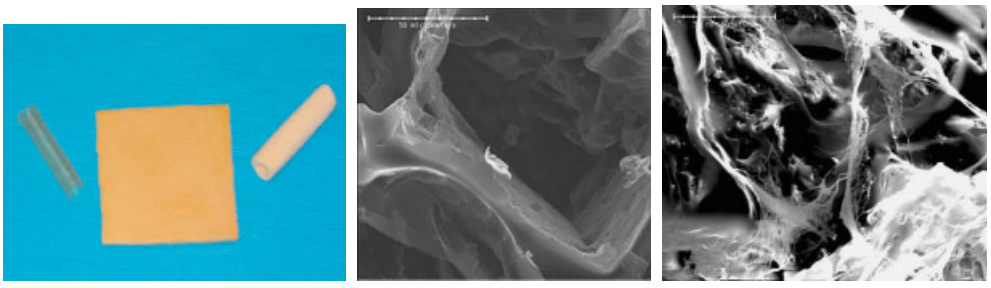

A) B) C)

Figure 3. A) Pictures of POC scaffolds (non-porous (left) and porous (right) tubes, and sponge (middle)); B) SEM of the porous POC scaffold cross section and C) SEM of HASMC cultured within a porous POC scaffold (1/1, 120 °C, vacuum, 3 days) for 4 weeks. Scale bars = 50 μm.

modulus was calculated. 4–6 samples were measured and averaged. The cross-link density (n) was calculated by equation (1) [4,30]:

$$n = \frac{E_0}{3RT} = \frac{\rho}{M_c} \quad (1)$$

where n represents the number of active network chain segments per unit volume; M_c represents the molecular weight between crosslinks (mol m^{-3}); E_0 represents Young's modulus (Pa); R is the universal gas constant (8.3144 J mol^{-1} K^{-1}); T is the absolute temperature (K); and ρ is the elastomer density (g m^{-3}) as measured via volume method [26].

In Vitro Degradation: Disk specimens (7 mm in diameter, approximately 1–1.5 mm thickness) were placed in a tube containing 10 ml phosphate buffer saline (pH 7.4) or 0.1 M NaOH to rapidly obtain relative degradation rates among samples. Specimens were incubated at 37 °C in PBS or NaOH for up to 26 weeks or 3 days, respectively. After incubation, samples were washed with water and dried under vacuum for 1 week. Mass loss was calculated by comparing the initial mass (W_0) with the mass measured at a given time point (W_t), as shown in Equation 2. Three individual experiments were performed for the degradation test. The results are presented as means ± standard deviation ($n = 3$).

$$\text{Mass loss}\,(\%) = \frac{W_0 - W_t}{W_0} \times 100 \quad (2)$$

Scaffold Fabrication and Characterization: POC pre-polymer was dissolved in dioxane at 25 wt.-% solution, followed by addition of sieved salt (90–120 μm), which served as a porogen. The resulting slurry was cast into poly(tetrafluoroethylene) (PTFE) molds (square and tubular shapes). For the burst pressure measurements, glass rods (~3 mm diameter) were subsequently coated with pre-polymer solution and air dried to allow for solvent evaporation. After solvent evaporation for 24 h, the mold or POC coated glass rods were transferred into a vacuum oven for post-polymerization (120 °C, vacuum, 3 days). The salt in the resulting composite was leached out by successive incubations in water (produced by Milli-Q water purification system, Billerica, MA, USA) every 12 h for 96 h. The resulting porous scaffold was air-dried for 24 h, vacuum dried for another 24 h, and then stored in a dessicator under vacuum before use. Scaffold cross-sections were observed by scanning electron microscopy (SEM, Hitachi 3500 N, EPIC, Northwestern University), and the images were analyzed using image analysis software (Image-Pro Plus V.4.0, Silver Spring, MD) to obtain the pore size data. Over fifty measurements were averaged to get the mean value and standard deviation of the pore size. The porosity of the scaffold was measured using a method based on Archimedes' principle as described elsewhere [26].

Fatigue resistance was assessed by monitoring the Young's modulus and dimensional recovery from deformation after compressing a cylindrical porous scaffold (6 mm height and 6 mm in diameter) five hundred times (at 2 mm min^{-1} at a maximum compressive strain of 60 % of original height with a 10 N load cell of an Instron 5544 mechanical tester).

In Vitro Biocompatibility Cell Culture: Human aortic smooth muscle cells (HASMC) and endothelial cells (HAEC) (Clonetics, Walkersville, MD) were cultured in a 50 ml culture flask with SmGM-2 and EBM-2 culture medium respectively (Clonetics, Walkersville, MD). Cell culture was maintained in a water-jacket incubator equilibrated with 5 % CO_2 at 37 °C. Cells were not used beyond passage five.

Cell Seeding on Polymer Films: POC films were cut into small pieces (1×2 cm^2) and placed in cell culture dishes (6 cm in diameter). All polymer samples were sterilized by incubation in 70 % ethanol for 30 min followed by UV light exposure for another 30 min. Approximately 30×10^4 HASMC or HAEC were added to a culture dish containing the POC film. The morphology of attached cells was observed and recorded with an inverted light microscope (Nikon Eclipse, TE2000-U) equipped with a Photometrics CoolSNAP HQ (Silver Spring, MD). Cell proliferation was assessed using the methylthiazoletetrazolium (MTT) assay for a period of 6 days. Briefly, POC thin films were cut into small disks (7 mm in diameter, 0.1 mm thick) with a cork borer and placed into the wells of a 96-well tissue culture plate. PLLA films (7 mm in diameter, 0.1 mm thick) and tissue culture polystyrene (TCPS) were used as controls. HASMC with a density of 3.13×10^3/well and HAEC (9.5×10^3/well) were added to each well (6 samples/day for each polymer type). The absorbance of formosan was measured as above.

Cell Seeding on Polymer Scaffolds: POC porous scaffolds were cut into small disks (7 mm in diameter, 1.5 mm of thickness) using a cork borer and placed in each well of a six-well plate. The disks were sterilized in a similar manner to the polymer films. HASMC (2×106/ml) were seeded within scaffolds by directly pipetting the cell suspension onto the scaffold. The cell-seeded scaffolds were maintained in the CO_2 incubator for 30 min at 37 °C, and then 5 ml of culture medium were added to the wells. The cell seeded scaffolds were fixed with 2.5 % glutaraldehyde in PBS for 24 h at 4 °C after cell culturing for 4 weeks. After being thoroughly washed with PBS, the scaffolds were dehydrated sequentially in 50, 70, 95, and 100 % ethanol each for 3×10 min. The fixed samples were freeze-dried, broken after freezing in liquid N_2, sputter-coated with gold, and examined under a scanning electron microscope (SEM, Hitachi 3500 N).

In Vivo Biocompatibility: POC disks (7 mm in diameter, 1.3 mm of thickness), sterilized via exposure to ethylene oxide gas, were implanted in seven-week-old female Sprague–Dawley rats by blunt dissection under deep isofluorane–O_2 general anesthesia. POC synthesized under different conditions (80 °C, no vacuum, 2 days; 80 °C, no vacuum, 2 weeks; 120 °C, vacuum, 3 days) was implanted symmetrically on the upper and lower back of the same animal. The rats were euthanized and tissue samples (3×3 cm) surrounding the implants were harvested with the intact implant at 60 days. The samples were fixed in 10 % formalin for 24 h and embedded in paraffin after a series of dehydration steps in ethanol and xylene. The slides were stained with hematoxylin and eosin (H&E).

POC Tube Burst Pressure Measurement: Burst pressure testing was performed by inflating POC tubes (3.65 mm inner diameter, 0.15 mm wall thickness) and recording the pressure at failure. A syringe pump (Sage Instruments, Boston, MA) with one 60 ml syringe was connected with Tygon tubing to one end of the POC tube while the other end was affixed with tubing to a pressure gauge (Cole Palmer, Vernon Hills, IL). The syringe pump was programmed to pump PBS at a rate of 0.67 ml min^{-1} through the tube while pressure was measured. Burst pressure was defined as the highest pressure value attained prior to failure.

Statistical Methods: Data are expressed as means ± standard deviation. The statistical significance between two sets of data was calculated using two-tail Student's t-test. Data were taken to be significant, when a P-value of 0.05 or less was obtained.

Received: October 10, 2003
Final version: December 18, 2003

[1] M. P. Lutolf, G. P. Raeber, A. H. Zisch, N. Tirelli, J. A. Hubbell, *Adv. Mater.* **2003**, *15*, 888.
[2] J. A. Rowley, Z. Sun, D. Goldman, D. J. Mooney, *Adv. Mater.* **2002**, *14*, 886.
[3] R. Langer, J. P. Vacanti. *Science* **1993**, *260*, 920.
[4] Y. D. Wang, G. A. Ameer, B. J. Sheppard, R. Langer, *Nat. Biotechnol.* **2002**, *20*, 602.
[5] S. H. Lee, B. S. Kim, S. H. Kim, S. W. Choi, S. I. Jeong, K. Kwon, S. W. Kang, J. Nikolovske, D. J. Mooney, Y. K. Han, Y. H. Kim, *J. Biomed. Mater. Res.* **2003**, *66A*, 29.
[6] J. P. Stegemann, R. M. Nerem, *Ann. Biomed. Eng.* **2003**, *31*, 391.
[7] R. M. Nerem, *Biorheology* **2003**, *40*, 281.
[8] M. Pei, L. A. Solchaga, J. Seidel, L. Zeng, G. Vunjak-Novakovic, A. I. Caplan, L. E. Freed, *FASEB J.* **2002**, *16*, 1691.
[9] S. D. Waldman, C. G. Spiteri, M. D. Grynpas, R. M. Pilliar, J. Hong, R. A. Kandel, *J. Bone Jt. Surg. Am. Vol.* **2003**, *9*, 9.
[11] R. Sodian, J. S. Sperling, D. P. Martin, A. Egozy, U. Stock, L. E. Mayer, J. P. Vacanti, *Tissue Eng.* **2000**, *6*, 183.
[12] R. Wada, S. H. Hyon, T. Nakamura, Y. Ikada, *Pharm. Res.* **1991**, *8*, 1292.

ADVANCED MATERIALS

[13] V. Maquet, S. Blacher, R. Pirard, J. P. Pirard, M. N. Vyakarnam, R. Jérôme, *J. Biomed. Mater. Res.* **2002**, *66*, 199.
[14] A. P. Pêgo, A. A. Poot, D. W. Grijpma, J. Feijen, *J. Controlled Release* **2003**, *87*, 69.
[15] J. Guan, M. S. Sacks, E. J. Beckman, W. R. Wagner, *J. Biomed. Mater. Res.* **2002**, *61*, 493.
[16] G. A. Skarja, K. A. Woodhouse, in *Polymers for Tissue Engineering* (Eds: M. S. Shoichet, H. A. Hubbell), VSP, Utrecht **1998**, p. 73.
[17] D. W. Urry, A. Pattanaik, J. Xu, T. C. Woods, D. T. McPherson, T. M. Parker, *J. Biomater Sci., Polym. Ed.* **1998**, *9*, 1010.
[18] J. S. Temenoff, K. A. Athanasiou, R. G. LeBaron, A. G. Mikos, *J. Biomed. Mater. Res.* **2002**, *59*, 429.
[19] J. A. Burdich, A. J. Peterson, K. S. Anseth, *Biomaterials* **2001**, *22*, 1779.
[20] K. T. Nguyen, J. L. West, *Biomaterials* **2002**, *23*, 4307.
[21] B. A. Nasseri, I. Pomerantseva, M. R. Kaazempur-Mofrad, F. W. H. Sutherland, T. Perry, E. Ochoa, C. A. Thompson, J. E. Mayer, S. N. Oesterle, J. P. Vacanti, *Tissue Eng.* **2003**, *9*, 291.
[22] J. Gosline, M. Lillie, E. Carrington, P. Guerette, C. Ortlepp, K. Savage, *Philos. Trans. R. Soc. London, Ser. B* **2002**, *357*, 121.
[23] M. C. Lee, R. C. Haut, *J. Biomech.* **1992**, *25*, 925.
[24] J. A. Hubbell, S. P. Massia, N. P. Desai, P. D. Drumheller, *Bio/Technology* **1991**, *9*, 568.
[25] A. G. Mikos, M. D. Lyman, L. E. Freed, R. Langer, *Biomaterials* **1994**, *15*, 55.
[26] J. Yang, G. X. Shi, J. Z. Bei, S. G. Wang, Y. L. Cao, Q. X. Shang, G. H. Yang, W. J. Wang, *J. Biomed. Mater. Res.* **2002**, *62*, 438.
[27] L. E. Niklason, J. Gao, W. M. Abbott, K. K. Hirschi, S. Houser, R. Marini, R. Langer, *Science* **1999**, *284*, 489.
[28] F. Barroso-Bujans, R. Martinez, P. Ortiz, *J. Appl. Polym. Sci.* **2003**, *88*, 302.
[29] J. Yang, J. Z. Bei, S. G. Wang, *Biomaterials* **2002**, *23*, 2607.
[30] L. H. Sperling, *Introduction to Physical Polymer Science*, John Wiley & Sons, New York **1992**.

A Multidye Nanostructured Material for Optical Data Storage and Security Data Encryption**

By *Hung H. Pham*, *Ilya Gourevich*, *Jung Kwon Oh*, *James E. N. Jonkman*, and *Eugenia Kumacheva**

Fast progress in information technologies triggers the need for new materials for high-density optical memory storage.[1–9] An increase in the number of molecular photosensitizers in a recording medium is a step towards a higher storage capacity: the number of recording modes in binary data storage scales as 2^n, where n is the number of photosensitizers that are individually addressed. For instance, using selective photobleaching of dyes, different data can be recorded and stored in the same spot of the recording medium. This strategy, however, has not found the attention it deserves: energy transfer leads to a cross-talk between the recorded data through quenching of dyes not directly addressed by irradiation. Here, we report a new approach to a multidye system for optical data storage and security needs. We employed core–shell particles comprised of different dyes in the core and in the shell to produce a multidye nanostructured material with a periodic structure. The incorporation of dyes in different phases of the material minimized energy transfer in the recording medium, while a highly regular structure of the material provided high-resolution recording. The composite material has promising applications as a medium for data storage in information technologies and as a storage medium for security purposes.

Figure 1a shows the approach used to create a multidye multiphase recording medium. The top cartoon shows a core–shell particle with two fluorescent dyes. Dye 1 is incorporated in the core-forming polymer (CFP) and dye 2 is localized in the shell-forming polymer (SFP). The specific relationship between the compositions of the CFP and the SFP provides the relationship $T_{g,SFP} < T_{g,CFP}$, where $T_{g,SFP}$ and $T_{g,CFP}$ are the glass-transition temperatures of the SFP and the CFP, respectively. Heat processing of a close-packed array of particles under conditions $T_{g,SFP} < T < T_{g,CFP}$ produces a two-phase film: a periodic array of spherical domains labeled with dye 1, which are embedded in a matrix containing dye 2. In a three-dye particle (Figure 1a, bottom cartoon) a rigid core contains dye 1, an inner shell (SFP-1) comprises dye 2, and an outer matrix-forming shell (SFP-2) carries dye 3. Annealing of the array of these microspheres at $T_{g,SFP\text{-}2} < T < T_{g,SFP\text{-}1} \leq T_{g,CFP}$ yields a material with three phases containing three different dyes. Selective photobleaching of dyes localized at the same spot of the two- or three-dye material yields four or eight storage modes, respectively, given that the size of a photoaddressed spot exceeds the size of a microsphere.

In the described strategy, the localization of dyes in different phases of the material can be achieved by covalent attachment of each dye to its hosting polymer and polymer cross-linking. The dimensions of the dye-labeled phases should be sufficiently large to be spatially resolved with optical techniques. For instance, for confocal fluorescence microscopy the lateral resolution (r_{xy}) is given by

$$r_{xy} \approx 0.4\lambda_{em}/NA \quad (1)$$

where λ_{em} is the emission wavelength and NA is the numerical aperture of the objective lens.[10] Finally, to avoid cross-talk, the dyes localized in different phases should have a sufficient spectral window.

We synthesized two types of core–shell particles: in the first system, particle cores and shells contained anthracene (An,

[*] Prof. E. Kumacheva, Dr. H. H. Pham, I. Gourevich, J. K. Oh
Department of Chemistry, University of Toronto
80 Saint George Street, Toronto, Ontario, M5S 3H6 (Canada)
E-mail: ekumache@chem.utoronto.ca
J. E. N. Jonkman
Advanced Optical Microscopy Facility, Ontario Cancer Institute
Princess Margaret Hospital
610 University Avenue
Toronto, Ontario, M5G 2M9 (Canada)

[**] The financial support of the Canada Research Chair Fund (NSERC Canada) and Premier Research Excellence Award is acknowledged with gratitude. We also wish to thank Prof. M. A. Winnik for useful discussions and Battista Calvieri and Steven Doyle for some of the bleaching experiments.

  DOI: 10.1002/adma.200306156